

CFD IMPELLER SPEED EVALUATION OF AN INDUSTRIAL SCALE TWO-PHASE FLOW STIRRED TANK

Tao SONG^{1,2}, Kaixi JIANG¹, Junwu ZHOU^{1,2}, Zhengchang SHEN¹, Yuqing FENG^{3*}

¹ Beijing General Research Institute of Mining and Metallurgy, Beijing 100160, CHINA

² Beijing Key Laboratory of Automation of Mining and Metallurgy Process, Beijing 102628, CHINA

³ CSIRO Mineral Resources Flagship, Clayton VIC 3168, AUSTRALIA

*Corresponding author, E-mail address: Yuqing.Feng@csiro.au

ABSTRACT

The industrial application of bio-oxidation in the gold extraction has been realized for years. The gold parceling in sulfides like pyrite and arsenopyrite could be exposed through bacterial oxidation pretreatment, and extracted with high recovery in the cyanidation. Large scale stirred tank bioreactors with high performance are essential to save operation costs for low grade refractory gold concentrates. In this paper, a gas-liquid two phase CFD model has been applied to investigate the air-water flow in an industrial scale bioreactor. The effects of the impeller speeds on tank performance are assessed in terms of the overall flow patterns, gas holdup, bubble residence time distribution, as well as water mixing. It was found that the water flow in the tank is dominated by stirred impellers with axial flow in the impeller zones. Small air bubbles generated by six gas nozzles distributed to the whole tank except the bottom area. The impeller speeds are essential to achieve a good gas-liquid flow pattern in the reactor. Simulation results obtained demonstrate the feasibility of the present modelling approach as a useful numerical tool to help potential improvement of industrial scale stirred tank bioreactor design and/or operation.

NOMENCLATURE

C_{μ}	bubble induced turbulent eddy viscosity coefficient
C_D	drag force coefficient
d	bubble diameter
g	gravity acceleration
k	turbulent kinetic energy
M	interfacial momentum transfer between phases
P	pressure
$S_{M\alpha}$	momentum sources due to external body forces
U	velocity
U_S	specified bubble terminal velocity
U_T	bubble terminal velocity
γ	volume fraction
ε	turbulent energy dissipation rate
ρ	density
∇	gradient operator
μ	dynamic viscosity
μ_{tc}	bubble induced turbulent eddy viscosity
μ_{td}	gas phase turbulent eddy viscosity
σ	turbulent Prandtl number
ν	continuous-phase kinematic viscosity

c	continuous liquid phase
d	dispersed gas phase
t	turbulence
α	phase, either gas (d) or water (c)

INTRODUCTION

Many gold deposits in China contain so-called refractory ore, where the gold is locked inside sulphides such as pyrite and arsenopyrite. These ores have to be specially treated to break down the sulphides before the gold can be extracted. This is conventionally done by roasting, necessitating substantial energy input and resulting in environmentally undesirable emissions, especially when dealing with arsenic minerals (Pinches, 2005). Pressure oxidation method is a more advanced refractory gold concentrates pretreatment. The hydro-process does not produce harmful gases, and can achieve a high gold exaction. However, the pressure oxidation process also need a high investment in facilities, maintains and trainings of the workers. Bio-oxidation technology uses the ability of certain microorganisms to oxidise sulphide minerals, an exothermal process from which these organisms gain energy. At the same time metals may be released into an aqueous solution. From 1980s, the gold concentrates tank bioleach has developed rapidly in the whole world. In last ten years, some biogold plants in China, such as Shandong Tarzan Biogold Company in Laizhou, Tianli Gold Plant in Liaoning, Jinfeng Biogold Plant in Guizhou, have been built, and high gold exactions and good environmental performances have been achieved (Yang *et al.*, 2002). This kind of modern, simple, cheap and environmentally sound technology is suitable for a large number of small gold mines in China, in which mostly contain refractory ores.

As the key facilities in gold bioleach plants, stirred tank bioreactors and airlift bioreactors are commonly used. In the main biogold company, such as Ashanti (Ghana), Fairview (Zambia), Sao Bento (Brazil), Wiluna (Australia), the stirred tank bioreactors are mainly used, and lead a good performance (Morin *et al.*, 2006). Bioreactors with high efficiency require proper flow fields for mineral particle suspension, low shear and nutrient environment for growth of bacteria, good bubble distribution for oxygen mass transfer. Scale-up of the high performance bioreactor is still a challenging task, especially for large-

scale reactors. Using CFD modelling, a wide range of variations in physical design and operational parameters can be tested and refined until a design that gives optimum performance. Nowadays, CFD models have been generally accepted as a powerful tool to assist designing new equipments and processes or process optimisation while minimising risk (Schwarz, 1994; Schwarz and Feng, 2014).

In this paper, a large scale stirred tank bioreactor with high performance designed by BGRIMM has been modeled. The CFD model was used to evaluate the performance of the bioreactor under several impeller speed conditions. The overall flow dynamics is investigated in terms of liquid velocity vectors. The relative performances have been evaluated in terms of gas holdup, bubble residence time distribution and liquid mixing.

MODEL DESCRIPTION

There are vast literatures on modelling techniques for gas liquid flows in stirred tanks (Bakker and van den Akker, 1994; Brucato et al., 1998; Aubin et al. 2004). Usually, the Eulerian-Eulerian model was found as a proper method in simulation of multiphase flow. The steady multiple reference frame (MRF) method and sliding mesh method were used to simulate impeller rotation. The Eulerian-Eulerian model requires less computing power than direct interface resolution, but the detailed bubbling hydrodynamics cannot be obtained. This model is still suitable for process simulation, and has been widely used in various multiphase flow systems (Schwarz and Turner, 1988; Lane et al., 2005).

The time averaged two-fluid (Euler-Euler) modelling approach has been adopted for this study. For the air-water system being studied in the stirred tank bioreactor, the equations are averaged over the phase structure so as to give time-averaged equations for each phase. The conservation of mass and momentum governing equations are summarized below:

$$\nabla \cdot (\gamma_\alpha \rho_\alpha U_\alpha) = 0 \quad (1)$$

$$\nabla \cdot (\gamma_\alpha (\rho_\alpha U_\alpha \otimes U_\alpha)) = -\gamma_\alpha \nabla P_\alpha + \quad (2)$$

$$\nabla \cdot (\gamma_\alpha \mu_\alpha (\nabla U_\alpha + (\nabla U_\alpha)^T)) + S_{M\alpha} + M_\alpha$$

Phase dependent turbulence models have been used, e.g. the dispersed phase zero equation model for the gas phase and the k-ε two-equation model for the liquid phase. In the liquid phase, an extra contribution to the turbulent viscosity due to bubble slip is included, following Sato and Sekoguchi (1975). The effective viscosity is a sum of the molecular and turbulent viscosities, with the turbulent eddy part calculated in:

$$\mu_{td} = \frac{\rho_d \mu_{tc}}{\rho_c \sigma} \quad (3)$$

$$\mu_{tc} = C_\mu \rho_c \frac{k_c^2}{\varepsilon_c} + 0.6 \rho_c \gamma_d d_d |U_d - U_c| \quad (4)$$

Coupling between the dispersed gas phase and continuum liquid phase is modelled using the drag law proposed by Fajner et al. (2008):

$$C_D = \frac{4 g d_d \rho_c - \rho_d}{3 U_s^2 \rho_c} \quad (5)$$

$$U_T = \left(2.14 \frac{\sigma}{\rho_c d_d} + 0.505 g d_d \right)^{0.5} \quad (6)$$

$$U_s = U_T \left\{ 0.32 \tanh \left[19 \frac{\lambda}{d_d} \left(\frac{|\rho_d - \rho_c|}{\rho_c} \right)^{0.5} - 1 \right] + 0.6 \right\} \quad (7)$$

Here $\lambda = (\nu^3/\varepsilon)^{0.25}$ is the Kolmogorov length. This model confirmed the significant role of turbulence in reducing the rising velocity of the buoyant particles and exhibited the same behaviour as the settling particles. The lift force describes the interaction of the bubble with the shear field of the liquid. This results in net force acting perpendicular to the motion of the bubble relative to the liquid on the bubble. Tomiyama (1998) lift force model was used here. A turbulence dispersion force is proposed to account for the diffusion of bubbles due to the random influence of turbulent eddies in the liquid using the Lopez turbulence dispersion force model (Lopez et al., 1994). In simulation, a steady-state model for the slurry and bubble flow within the tank was solved first. Then, by holding the gas-liquid flow field fixed, a transient model of two additional variables were used to predict the time varying of bubbles and slurries in the tank. The transport equation for the two variables followed:

$$\frac{\partial(\rho\varphi)}{\partial t} + \nabla \cdot (\rho U \varphi) = \nabla \cdot \left[\left(\rho D_\varphi + \frac{\mu_t}{\sigma_{tc}} \right) \nabla \varphi \right] + S_\varphi \quad (8)$$

which were set the respective properties of gas and liquid to track the flow of bubbles and slurries separately.

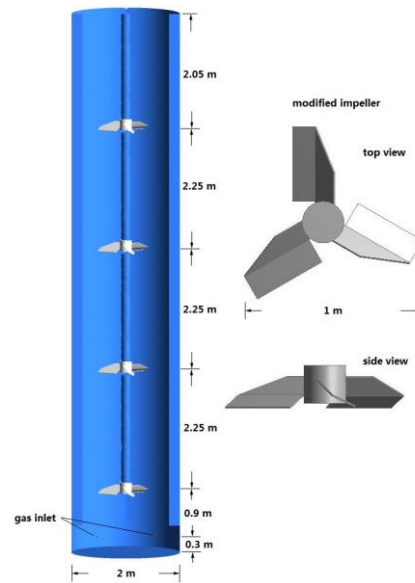


Figure 1: The geometry of this industrial stirred tank bioreactor.

The stirred tank bioreactor designed for refractory gold ores by BGRIMM is a kind of baffled tank with multiple impellers. The impeller is designed to be an axial flow impeller and is similar to hydrofoil impeller. The diameter of the impeller is 1 m, and each impeller has 3 blades. At the bottom of tank, there are 6 high speed gas nozzles, which can generate small bubbles, installed evenly at the side wall 0.3 m above the flat tank bottom. The height of the tank is 10 m with an internal diameter of 2 m. The total volume of the reactor is 31.4 m³. The default design has 4 impellers installed, and bottom clearance is 0.9 m. The interval between impellers are 2.25 m. The distance between the top impeller the free liquid surface is 2.05 m. Figure 1 shows the geometry structure of the impeller and this stirred tank bioreactor.

The CFD model has been setup using the geometry of the full-scale bioreactor. In this study, only water and air were considered for industrial experiments in water environment. The simulations were tested under two different mesh sizes. The fine grid included 692,278 cells. The coarse structural grid was 373,129 cells. The differences between simulation results of gas volume fraction in the whole tank under two kinds of grids were less than 4%. Considering the computing time, the coarse mesh was used in this paper.

A commercial CFD code ANSYS CFX14.5 has been used to obtain a solution of the above equations. A gas outlet boundary condition has been used on the top surface of the stirred tank bioreactor through which gas leaves the tank at the rate it arrives from below (an option called “degassing condition” in CFX). Wall solid boundaries were set as no slip for water and free slip for air.

RESULTS

In the bioreactor, hydrofoil impellers were developed for applications where axial flow is important and low shear is desired. For the practice in bacteria bio-oxidation process this type of impeller is proper to generate circulation flow and bubble distribution. A low shear environment is also good for growth of bacteria. In the reactor, bubble size was assumed to be in a uniform size of 2 mm, which was based on observation of the gas nozzle experiments in laboratory. Several simulations were conducted to test the effect of impeller speed of 0, 16, 32 and 48 rpm, and the gas flow rates were all $0.3 \text{ m}^3\text{m}^{-2}\text{min}^{-1}$.

Figure 2 and Figure 3 show the water and air velocity distribution along the middle vertical plane under different impeller speeds. When the impeller speed was 0 rpm, the injected bubbles rose up directly to the free surface due to the buoyancy force, and the water moved to the vacancy where bubble left. So no regular circulation was generated in the bioreactor. When the impeller speed increased, axial flow circulations were generated near the impeller areas. In the same time, air bubbles near impeller zones were also dragged into the swirls and moved along the circulation routes.

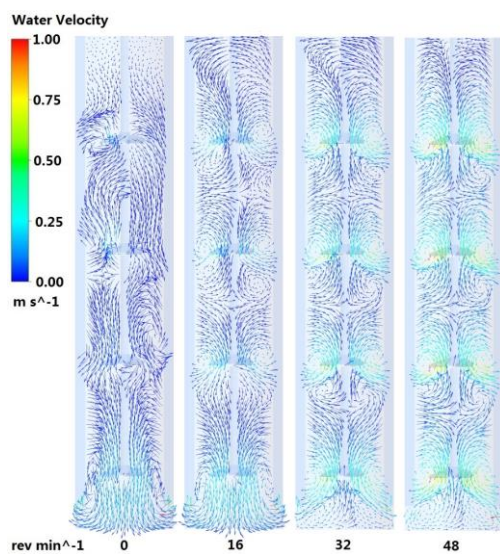


Figure 2: Water velocity vectors in the middle slice plane for different impeller speeds under the gas flow rate of $0.3 \text{ m}^3\text{m}^{-2}\text{min}^{-1}$.

Figure 4 predicts gas volume fraction under 4 different impeller speed. When the impeller did not spin, the gas volume fraction was apparently smaller. As the increase of the impeller speed, air bubble moved to more area in the tank. But there is nearly no gas in the bottom of the reactor.

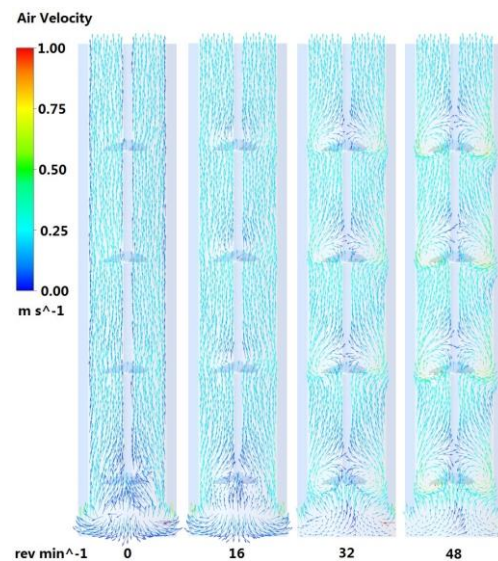


Figure 3: Gas velocity vectors in the middle slice plane for different impeller speeds under the gas flow rate of $0.3 \text{ m}^3\text{m}^{-2}\text{min}^{-1}$.

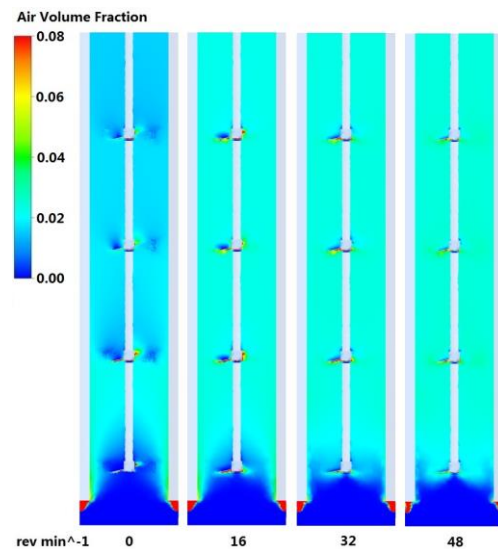


Figure 4: Gas volume fraction in the middle slice plane for different impeller speeds under the gas flow rate of $0.3 \text{ m}^3\text{m}^{-2}\text{min}^{-1}$.

The shear strain rate at some point within the material measures the rate at which the distances of adjacent parcels of the material change with time in the neighborhood of that point. It reflects the rate at which it is being deformed by progressive shearing without changing its volume. It is zero if these distances do not change, as happens when all particles in some region are moving with the same velocity (same speed and direction) and/or rotating with the same angular velocity, as if that part of the medium were a rigid body. When the impeller speed increases, velocity difference turns to be bigger in the rotational area, and brings higher shear which is harmful for the bacteria in bio-oxidation process. Figure 5

shows the simulated shear strain rates under 4 different impeller speeds. Higher impeller speed brought higher shear strain rate in the interaction zones. Although mechanical destruction of bacteria has been noticed under various operating conditions, the amount of shear at the onset of cell damage has not been quantified for bio-oxidation (Bailey and Hansford, 1992). Hack et al. (1989) found low leach rates were caused by excessive shear stress during the pilot plant test work. Leaching was improved when impeller tip speed was reduced from 5.3 m/s to 3.3 m/s. In this work, when the impeller speed was 48 rpm, the tip speed was nearly 2.5 m/s. Taking the research results proposed by Hack et al. (1989) as reference, the impeller speed of 32 and 48 rpm are all acceptable for the leaching process.

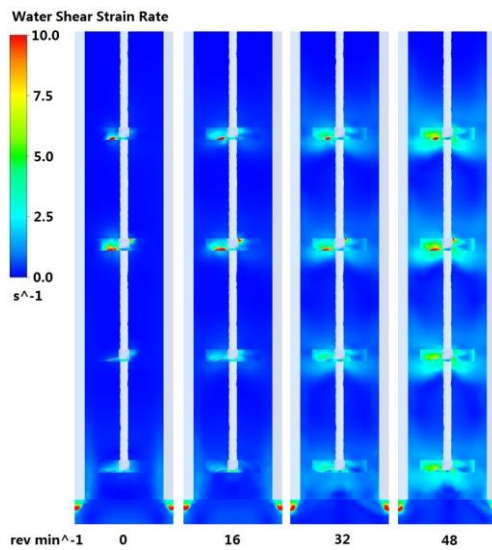


Figure 5: Water shear strain rate in the middle slice plane for different impeller speeds under the gas flow rate of $0.3 \text{ m}^3\text{m}^{-2}\text{min}^{-1}$.

In the present bacteria bio-oxidation operation, a certain amount of gas holdup is required to ensure the oxygen and carbon dioxide mass transfer between air bubble and liquid phase, and the bubble residence time should be as long as possible to increase the reaction speed and feed the microorganism. Checking the bubble residence time distribution (RTD) could present the bubble residence time in the bioreactor. The bubble RTD is calculated by step tracer methods, e.g. continuously injecting bubble tracers from the gas inlet and monitoring gas escaping rate from the tank top. Once the bubble tracers reach a dynamically stable state, e.g. the bubble escaping rate is equivalent to the gas injection rate, the bubble RTDs can be obtained. Figure 6 compares the calculated bubble RTD density curves under different impeller speeds. The bubble RTD density curves in the bioreactor used here were similar to log normal distribution density curves. When there was no impeller spin, the mean of bubble RTD density curve was smaller than the conditions when impeller spun. When the impeller was 16 rpm, the peak value was a little bigger than the conditions when the impeller speeds were 32 and 48 rpm. Under the impeller speed of 32 and 48 rpm, the mean and the standard deviation of the distributions were similar to each other, but the peak value was smaller than the condition when the impeller speed was 16 rpm. Taken the consideration of Figure 7a and Figure 7b, which quantitatively present the

gas volume fraction and mean bubble residence time, the mean bubble residence time is linearly proportional to the gas holdup.

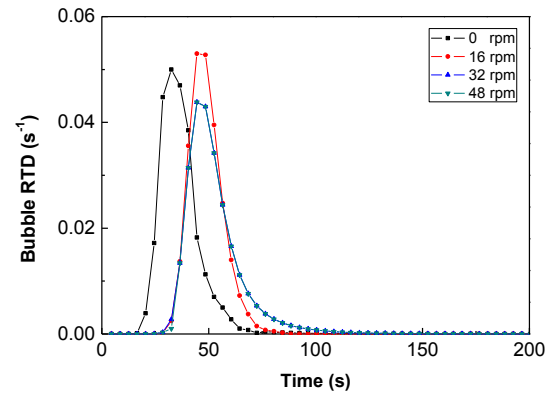


Figure 6: RTD curves for the step input bubble tracer for different impeller speeds under the gas flow rate of $0.3 \text{ m}^3\text{m}^{-2}\text{min}^{-1}$. (the curve of 32 rpm coincides with the curve of 48 rpm)

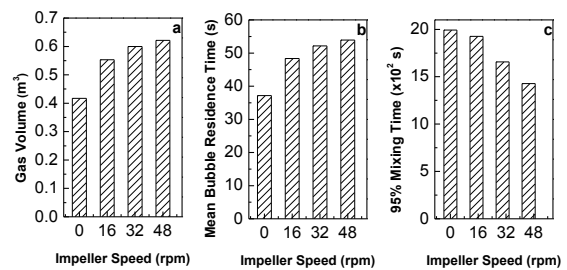


Figure 7: Simulation results for different impeller speeds under the gas flow rate of $0.3 \text{ m}^3\text{m}^{-2}\text{min}^{-1}$: (a) gas volume in tank; (b) mean bubble residence time; (c) 95% mixing time.

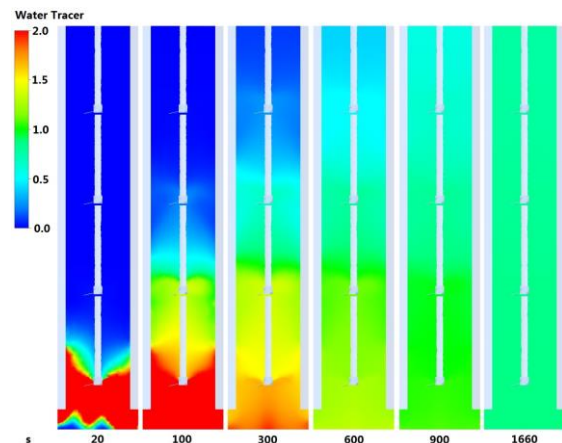


Figure 8: Water tracer distributions in the leaching tank under impeller speed of 32 rpm and gas flow rate of $0.3 \text{ m}^3\text{m}^{-2}\text{min}^{-1}$ after 20s, 100s, 300s, 600s, 900s and 1660s.

The level of liquid mixing is an important parameter to assess the tank performance. Pulse water tracers are put into the leaching tank from the slurry inlet located at the bottom area to evaluate the mixing behavior of the bioreactor. Figure 8 shows the water tracer distributions over a vertical plane in the bioreactor under impeller speed of 32 rpm and gas flow rate of $0.3 \text{ m}^3\text{m}^{-2}\text{min}^{-1}$. After the injection, the water tracers flow upward, and disperse in a

wider region. Before evenly distributing in the tank, the tracer experiences a dispersion from the bottom to the top area in the reactor. After about nearly 1660 seconds, an almost uniform distribution of slurry is achieved. For the other three impeller speeds, the tracer mixing pattern are very similar, thus, their temporal-spatial distribution are not plotted. The 95% mixing time are presented in Figure 7c, decreasing with the increased impeller speed.

CONCLUSION

Air-water flow in a bio-oxidation reactor for refractory gold ore has been investigated using a gas-liquid two phase CFD model with ANSYS CFX14.5 being the numerical platform. The likely effects of the impeller speed, the impeller installation condition and gas flow rates on tank performance are assessed in terms of the overall flow patterns, gas holdup, bubble residence time distribution, as well as the water mixing. The impeller rotation is the main mixing power input in this bioreactor. The impeller speed is the decisive factor for the flow pattern of air and liquid, and also for the mass transfer and the particle suspension. The impeller speed of 32 and 48 rpm showed better performance than the speed of 0 and 16 rpm, and presented similar gas volume fraction and bubble RTD. So these two speed settings are recommended in this study. Simulation results obtained demonstrate the feasibility of the present modelling approach as a useful numerical tool to help understanding the influence of impeller settings and gas flow rates for the bioreactor. Further work with the consideration of oxygen/dioxide mass transfer between the air and water/slurry will be performed under a wider design/operation conditions to fully clarify this issue in detail.

REFERENCES

- AUBIN J., FLETCHER D.F., XUERE B. C., (2004), "Modeling turbulent flow in stirred tanks with CFD: the influence of the modeling approach, turbulence model and numerical scheme", *Experimental Thermal Fluid Science*, **28**, 431-445.
- BARIGOU M., GREAVES M., (1992), "Bubble-size distributions in a mechanically agitated gas-liquid contactor", *Chemical Engineering Science*, **47(8)**, 2009-2025.
- BAKKER A., VAN DEN AKKER H.E.A., (1994), "A computational model for the gas-liquid flow in stirred reactors", *Chem. Eng. Res. Des.*, **72**, 594-606.
- BRUCATO A., CIOFALO M., GRISAFI F., MICALE G., (1998), "Numerical prediction of flow fields in baffled stirred vessels: A comparison of alternative modelling approaches", *Chemical Engineering Science*, **53(21)**, 3653-3684.
- FAJNER D., PINELLI D., GHADGE R.S., MONTANTE G., PAGLIANTI A., MAGELLI F., (2008), "Solids distribution and rising velocity of buoyant solid particles in a vessel stirred with multiple impellers", *Chemical Engineering Science*, **63(24)**, 5876-5882.
- FENG Y.Q., YANG W., COOKSEY M., SCHWARZ M.P., (2010), "Development of Bubble Driven Flow CFD Model Applied for Aluminium Smelting Cells", *The Journal of Computational Multiphase Flows*, **2(3)**, 179-188.
- HACK R.P., WRIGHT F.R., GORMLEY L.S., (1989), "Bioleaching of refractory gold ores-Out of the lab into the plant", J. Salley, R. G. L. McCready, and P. L. Wichlacz (eds.), *Biohydrometallurgy, International Symposium Proceedings*, Jackson Hole, Wyoming. Canadian Centre for Mining and Energy Technology, Canada, 533-550.
- LOPEZ DE BERTODANO M., LAHEY R.T., JONES O.C., (1994), "Development of a k-ε model for bubbly two-phase flow", *Journal of Fluid Engineering*, **116(1)**, 128-134.
- LANE, G.L., SCHWARZ, M.P., EVANS, G.M., (2005), "Numerical modelling of gas-liquid flow in stirred tanks", *Chemical Engineering Science*, **60**, 2203-2214.
- MORIN D., LIPS A., PINCHES T., HUISMAN J., FRIAS C., NORBERG A., FORSSBERG E., (2006), "BioMinE - Integrated project for the development of biotechnology for metal-bearing materials in Europe", *Hydrometallurgy*, **83(1-4)**, 69-76.
- PINCHES T., (2005), "Bacteria mines' new best friend", *Mining Mirror*, **Dec**, 24-29.
- SATO Y., SEKOGUCHI K., (1975), "Liquid Velocity Distribution in Two-Phase Bubble Flow", *International Journal of Multiphase Flow*, **2(1)**, 79-95.
- SCHWARZ, M.P. and TURNER, W.J., (1988), "Applicability of the standard k-ε turbulence model to gas-stirred baths", *Appl. Math. Modelling*, **12**, 273-279.
- SCHWARZ, M.P., (1994), "The role of computational fluid dynamics in process modeling", 6th AusIMM Extractive Metallurgy Conf., 31-36.
- SCHWARZ, M.P. and FENG, Y.Q., (2014), "Complex multiphase applications of CFD", 10th International Conference on CFD in Oil & Gas, Metallurgical and Process Industries, June 17-19, SINTEF, Trondheim, Norway.
- TOMIYAMA A., (1998), "Struggle with computational bubble dynamics", *Multiphase Science and Technology*, **10(4)**, 369-405.
- YANG S.R., XIE J.Y., QIU G.Z., HU Y.H., (2002), "Research and application of bioleaching and biooxidation technologies in China", *Minerals Engineering*, **15(5)**, 361-363.
- YANG N., CHEN J.H., ZHAO H., GE W., LI J.H., (2007), "Explorations on the multi-scale flow structure and stability condition in bubble columns", *Chem. Eng. Sci.*, **62(24)**, 6978-6991.
- YANG N., CHEN J.H., GE W., LI J.H., (2010), "A conceptual model for analyzing the stability condition and regime transition in bubble columns", *Chem. Eng. Sci.*, **65(1)**, 517-526.
- YANG N., WU Z.Y., CHEN J.H., WANG Y.H, LI J.H., (2011), "Multi-scale analysis of gas-liquid interaction and CFD simulation of gas-liquid flow in bubble columns", *Chem. Eng. Sci.*, **66(14)**, 3212-3222.
- ZADGHAFARI R., and MOGHADDAS J.S., (2010), "Evaluation of drag force effect on hold-up in a gas-liquid stirred tank reactor", *Journal of Chemical Engineering of Japan*, **43(10)**, 833-840.
- ZHANG K.Y., FENG Y.Q., SCHWARZ P. M., WANG Z.W., COOKSEY M., (2013), "Computational fluid dynamics (CFD) modeling of bubble dynamics in the aluminum smelting process", *Ind. Eng. Chem. Res.*, **52(33)**, 11378-11390.